Arthropod Structure & Development 40 (2011) 128–134

Contents lists available at ScienceDirect

Arthropod Structure & Development

journal homepage: www.elsevier.com/locate/asd

# The properties of the visual system in the Australian desert ant *Melophorus bagoti*

Sebastian Schwarz [a,*], Ajay Narendra [b], Jochen Zeil [b]

[a] Department of Brain, Behaviour and Evolution, Macquarie University, Sydney, NSW 2109, Australia
[b] ARC Centre of Excellence in Vision Science and Centre for Visual Sciences, Division of Ecology, Evolution and Genetics, Research School of Biology, The Australian National University, Canberra, ACT 0200, Australia

ARTICLE INFO

*Article history:*
Received 29 June 2010
Accepted 20 October 2010

*Keywords:*
Compound eye
Ommatidia
Insect vision
Resolution
Visual field
*Melophorus bagoti*

ABSTRACT

The Australian desert ant *Melophorus bagoti* shows remarkable visual navigational skills relying on visual rather than on chemical cues during their foraging trips. *M. bagoti* ants travel individually through a visually cluttered environment guided by landmarks as well as by path integration. An examination of their visual system is hence of special interest and we address this here. Workers exhibit distinct size polymorphism and their eye and ocelli size increases with head size. The ants possess typical apposition eyes with about 420–590 ommatidia per eye, a horizontal visual field of approximately 150° and facet lens diameters between 8 and 19 μm, depending on body size, with frontal facets being largest. The average interommatidial angle $\Delta\phi$ is 3.7°, the average acceptance angle of the rhabdom $\Delta\rho_{rh}$ is 2.9°, with average rhabdom diameter of 1.6 μm and the average lens blur at half-width $\Delta\rho_l$ is 2.3°. With a $\Delta\rho_{rh}/\Delta\phi$ ratio of much less than 2, the eyes undersample the visual scene but provide high contrast, and surprising detail of the landmark panorama that has been shown to be used for navigation.



## 1. Introduction

The most common mechanisms by which ants find their way to food sites or back to the nest are by following a scent trail, by relying on path integration and/or on landmark guidance. The primary means of navigation for ants that live in landmark-poor desert environments is path integration, a strategy that allow ants to take the shortest possible path back home after a circuitous foraging trip (Collett and Collett, 2000; Wehner, 2003). In landmark-rich environments ants rely more heavily on visual landmark information (Beugnon et al., 2001; Fukushi, 2001; Narendra, 2007b; Bregy et al., 2008). Visual landmarks are used to locate specific goals (Wehner and Räber, 1979; Collett, 1992; Macquart et al., 2006), to follow routes (Collett et al., 1992; Graham et al., 2003; Narendra, 2007b; Wystrach et al., 2010) and to determine compass directions. For both path integration and landmark guidance ants make use of a variety of compass cues: the pattern of the polarised skylight (Duelli and Wehner, 1973), the position of the sun (Wehner and Müller, 2006), the landmark panorama (Fukushi, 2001; Graham and Cheng, 2009a,b), the pattern of the canopy (Hölldobler, 1980) and possibly also the direction of the magnetic field (Çamlitepe and Stradling, 1995; Riveros and Srygley, 2008).

Foragers of the Australian desert ant *Melophorus bagoti* scavenge mainly for other arthropods that have fallen victim to the heat of the desert sun (Muser et al., 2005; Schultheiss et al., 2010). Individual ants leave their nest for relatively long foraging trips and locate the nest on their return with high precision. *M. bagoti* are visually guided ants that localise goals using landmarks (Narendra et al., 2007), follow landmark-defined routes (Kohler and Wehner, 2005; Narendra, 2007b) and use the distant landmark panorama as a compass cue (Graham and Cheng, 2009a). The extent to which they rely on visual landmarks depends on their familiarity with a scene (Narendra, 2007a,b).

Little is known, however, about the properties of the visual system in *M. bagoti*. As we show here, the ants possess apposition compound eyes, which are typical for insects with diurnal lifestyle (Land and Nilsson, 2002). In apposition compound eyes, light reaches the fused rhabdom to which all photoreceptor cells contribute through one individual corneal lens. The number, arrangement and dimensions of ommatidia determine the visual field and the resolution (acuity) of compound eyes.

In this study we analyse the behaviourally relevant properties of the compound eyes of *M. bagoti* as far as resolving power is concerned, the distribution of facet size across the eye and note the unusual presence and the external dimensions of the ocelli.

## 2. Materials and methods

*Melophorus bagoti* (Lubbock) foragers were collected from different nests about 10 km south of Alice Springs, NT. Head width, compound eye and ocelli size were measured from photographs

* Corresponding author. Tel.: +61 2 98504189; fax: +61 2 98509231.
*E-mail addresses:* sebastian.schwarz@mq.edu.au (S. Schwarz), ajay.narendra@anu.edu.au (A. Narendra), jochen.zeil@anu.edu.au (J. Zeil).

1467-8039/$ – see front matter © 2010 Elsevier Ltd. All rights reserved.
doi:10.1016/j.asd.2010.10.003

taken with a dissection Zeiss microscope (8-32×). To determine the exact number and size distribution of facet lenses, we covered compound eyes with a thin layer of colourless nail polish to produce cornea replicas (Ribi et al., 1989). Once dry, the cornea replicas were carefully removed and flattened on a microscope slide by making incisions with a micro-scalpel. Photographs of the replicas were taken in a Zeiss light microscope with a 5× objective. A custom written program (Richard Peters, La Trobe University) in Matlab®2009 (MathWorks, Inc., Natick, Massachusetts, USA) allowed us to mark each facet in the digital photographs of these replicas and determine their area. From this we created maps of the facet array and determined the distribution of facet sizes. We used one of the largest workers to develop an eye map.

For the examination of the fine structure of the compound eye animals were processed following conventional histological methods (Sabatini et al., 1963). The eyes were fixed during the day, which corresponds to the activity times of *M. bagoti*. Ants were immobilized on ice, their mandibles were removed and the head capsules opened. Optimal retinal fixation was achieved by cutting the most ventral rim of the eye. Eyes were fixed for 2 h in a mixture of 2.5% glutaraldehyde and 2% paraformaldehyde in phosphate buffer (pH 7.2–7.5), followed by a series of buffer washes and post-fixation in 2% $OsO_4$ in distilled water for 2 h. The heads were then dehydrated in an ethanol series, transferred to acetone and embedded in Epoxy resin (FLUKA). One-micron thick serial longitudinal and cross-sections of ommatidia of the eye were cut on a Reichert Ultracut microtome using glass knives. Sections for light microscopy were stained with toluidine blue and digitally photographed with a Zeiss photo-microscope.

To estimate the spatial resolution in *M. bagoti* we calculated the interommatidial angle ($\Delta\phi$) by measuring in digital photographs of histological sections the local eye radius ($R$) from segments with baseline length ($s$) and height ($h$) (Fig. 1A).

$$r = \frac{(s/2)^2 + h^2}{2h}.$$

Interommatidial angles ($\Delta\phi$) were then determined (Land, 1997) from the diameter of the corneal lens ($A$) and the eye radius ($R$) according to:

$$\Delta\phi = A/R$$

The approximate angular acceptance function of rhabdoms was estimated by determining the lens blur, given by the half-width of the Airy Disk $\Delta\rho_l = \lambda/A$, with $\lambda$ = wavelength of green light (0.5 μm) and the angular extent of the rhabdom at the nodal point of the lens, given by $\Delta\rho_{rh} = d/f$, with $d$ = diameter of the distal tip of the rhabdom and $f$ = focal length (note that all the angular values are in radians). According to Stavenga (2003a), $\Delta\rho_{rh}$ provides the best estimate of the true acceptance function of small diameter rhabdoms. We determined the effective focal length by applying the thick lens formula (see Stavenga, 2003b), with the power of the thick lens

$$P_L = P_1 + P_2 + P_3,$$

where

$$P_1 = \frac{n_1 - n_0}{r_1},\quad P_2 = \frac{n_2 - n_1}{r_2},\quad P_3 = -\frac{t}{n_1}P_1P_2.$$

with $P_1$, the power of the front surface of the lens, $P_2$, the power of the back surface of the lens and refractive indices for air $n_o = 1$; for the lens $n_1 = 1.43–1.45$; for the crystalline cone $n_2 = 1.34$; $r_1$ = outer lens surface radius; $r_2$ = inner lens surface radius and $t$ = the distance between the vertices of the inner and outer lens surface (the thickness or length of the lens; see Fig. 1B).

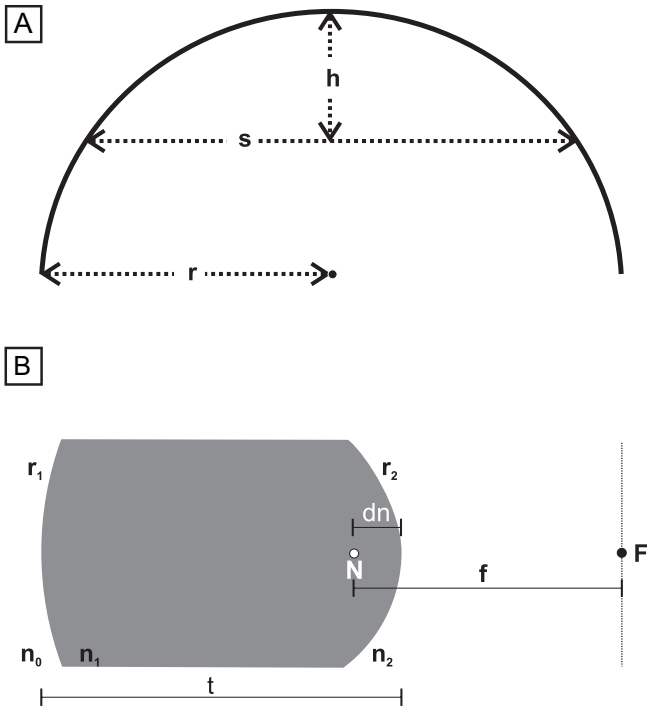


**Fig. 1.** (A) Schematic drawing to illustrate how the local eye radius ($r$) was determined from the length of a segment ($s$) transecting the eye and its height ($h$). (B) Properties of a thick lens that are required to determine its effective focal length ($f$) measuring the distance between the back nodal point ($N$) and the focal plane ($F$), with light assumed to enter from the left. $n_0$, $n_1$, $n_2$ are the refractive indices of air, lens and crystalline cone, respectively. ($r_1$) is the radius of curvature of the outer, ($r_2$) of the inner lens surface and ($t$) is the thickness of the corneal lens measured as the distance between the two vertices. The distance of the nodal point ($N$) from the back vertex is denoted by ($dn$).

The primary focal length $f$ (see Fig. 1B) as measured from the secondary nodal point $N$ is

$$f = n_0/P_L$$

and the distance $dn$ of the secondary nodal point $N$ from the vertex of the back surface of the lens (Fig. 1B) is given by

$$dn = \frac{n_2(1 - tP_1/n_1)}{P_L} - f.$$

## 3. Results

### 3.1. Overview

There is a clear size polymorphism among workers of *M. bagoti*, with head width measuring 1.7 mm in smallest and 3.2 mm in largest workers (Christian and Morton, 1992). Workers possess two compound eyes and three ocelli. The left and right compound eye are of equal size (anterior–posterior axis: $t$ test, $p = 0.15$; dorsal–ventral axis: $t$ test, $p = 0.46$). However, eye size increases with head size (anterior–posterior axis: Pearson correlation test, $r = 0.930$, $p < 0.001$; dorsal–ventral axis: Pearson correlation test, $r = 0.748$, $p < 0.001$; Fig. 3A and B). The ocelli are located on the dorsal central region of the head between the compound eyes (Fig. 2C). The size of the median ocellus increases with head size (Pearson correlation test, $r = 0.705$, $p = 0.01$; Fig. 3C).

### 3.2. Facet number, size and distribution

Workers of *M. bagoti* possess between 421 and 590 facets per eye (Table 1), with the number of facets significantly correlated

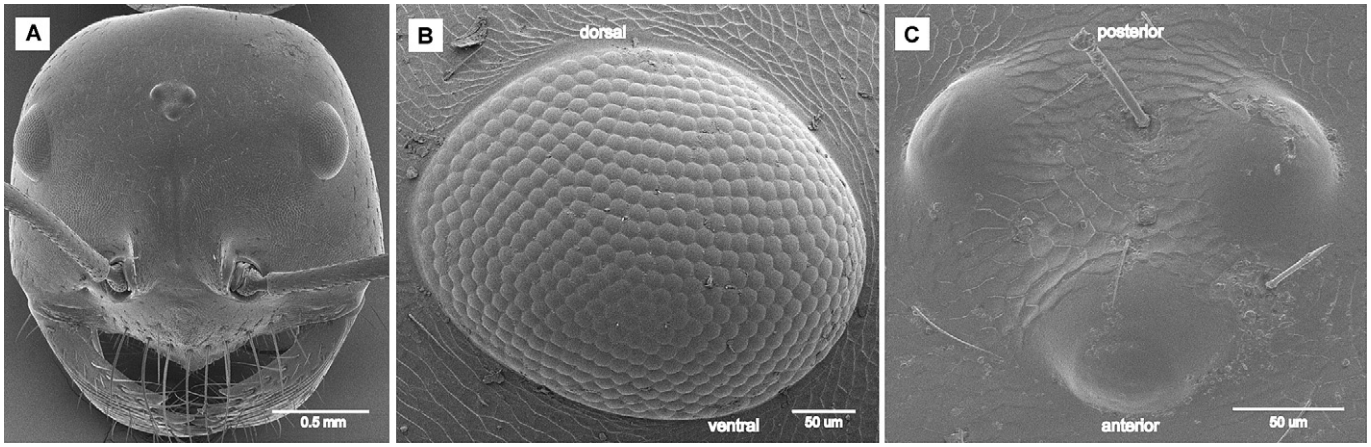


**Fig. 2.** External morphology of the *M. bagoti* head. (A) Scanning electron microscope (SEM) photograph of a worker. The compound eyes are located towards the frontal lateral side. (B) A SEM close-up of the right compound eye with between 421 and 590 ommatidia depending on the size of the ant. (C) Three ocelli lie dorsally between the compound eyes.

with head size (Pearson correlation test, $r = 0.705$, $p = 0.01$; Fig. 3D). The eyes are elongated in the horizontal direction so that in large workers, about 30 ommatidia lie along the eye equator as compared to 26 in dorsal–ventral direction (see Fig. 2B). Facet diameters range from 8 to 13 μm in small (SD: 1.89, $N = 100$, average: 12.3 μm) and 13–19 μm in large ants (SD: 2.20, $N = 80$, average: 13.4 μm). They are quite uniformly distributed across the eye, with a slight gradient from anterior (facet area: 250–300 $\mu m^2$) to posterior (facet area: 150–200 $\mu m^2$; Fig. 4).

### 3.3. Optical properties

The average interommatidial angle ($\Delta\phi$) is 3.7°, as calculated with the average diameter of the facet lenses (12.6 μm) and the overall horizontal eye radius of 195 μm (see Table 1). However, eye shape is not uniform across the visual field (Fig. 4, Table 1) with the local eye radius varying from 156 μm in the anterior, through 179 μm in the lateral to 245 μm in the posterior eye and facet lens diameters being slightly larger in the front than in the back. Along

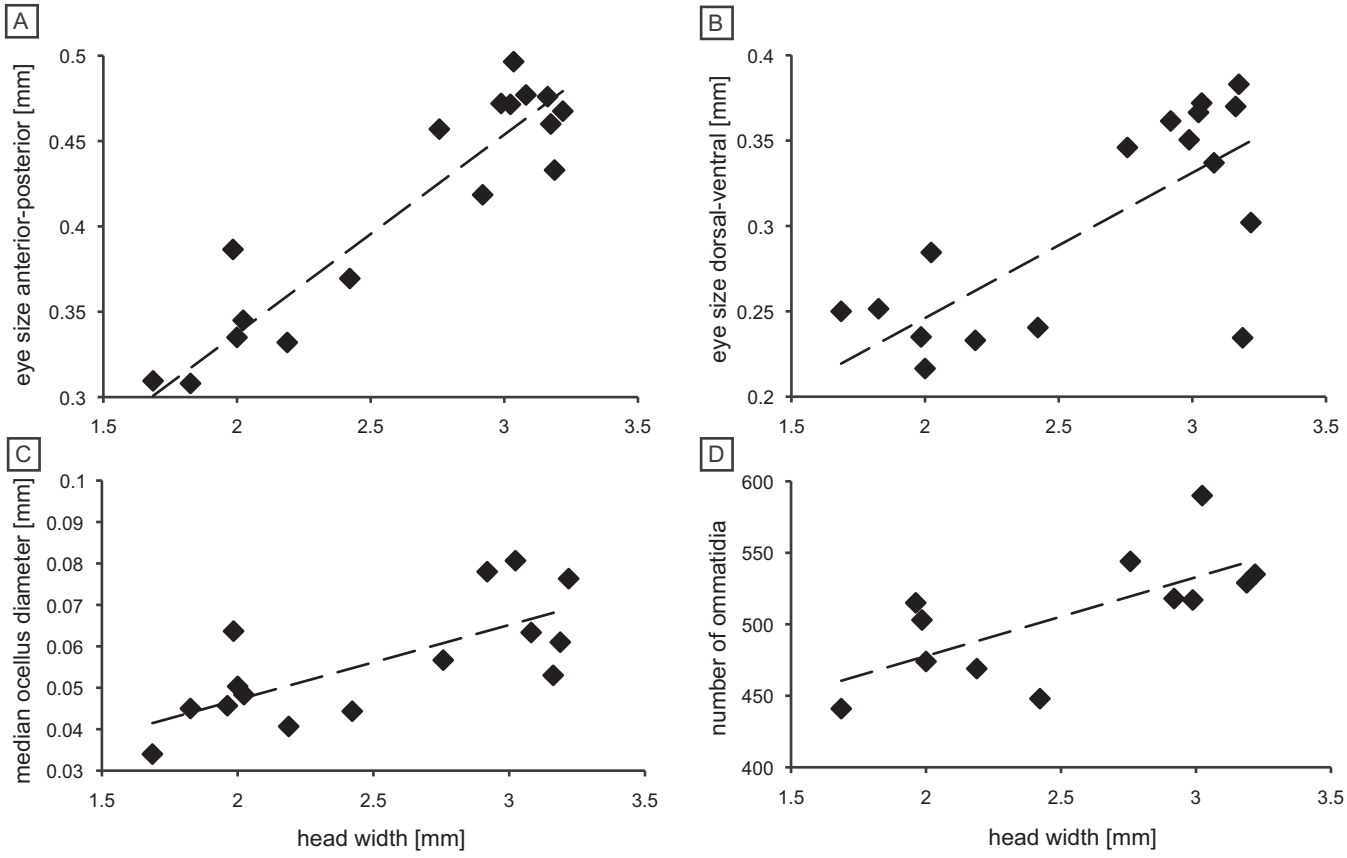


**Fig. 3.** The relationship between head width, the size of the compound eye and the size of the median ocellus. Plotted against head width are (A) the anterior – posterior eye length; (B) the dorsal – ventral eye length; (C) the size of the median ocellus; and (D) the number of ommatidia. See text for details and statistics.

**Table 1**
Summary of morphological and histological measurements in *M. bagoti*. For each measurement, the number of samples (N), the range and the average are given. In addition, for the dimensions of rhabdom diameters, the depth of the sections in which the measurements were made are given in microns (CS = cross section).

| | *N* | Range | Average |
|---|---|---|---|
| Head width [mm] | 18 | 1.7–3.2 | 2.6 ± 0.6 |
| Head length [mm] | 18 | 1.6–2.7 | 2.2 ± 0.4 |
| Eye anterior–posterior [mm] | 18 | 0.3–0.5 | 0.4 ± 0.1 |
| Eye dorsal–ventral [mm] | 18 | 0.2–0.4 | 0.3 ± 0.1 |
| Median ocellus size [mm] | 15 | 0.03–0.1 | 0.1 ± 0.01 |
| Facet diameter [μm] | 180 | 7.9–19.3 | 12.6 ± 0.9 |
| Facet number | 13 | 421–590 | 499 ± 43.2 |
| Eye radius – whole eye [μm] | 3 | 194.6–195.2 | 195.0 ± 0.3 |
| Eye radius – frontal [μm] | 3 | 151.5–162.9 | 155.8 ± 6.2 |
| Eye radius – lateral [μm] | 3 | 162.6–188.3 | 179.2 ± 14.4 |
| Eye radius – posterior [μm] | 3 | 232.9–249.8 | 242.9 ± 8.9 |
| Thickness of corneal lens [μm] | 25 | 15.7–21.1 | 18.7 ± 1.1 |
| Outer lens radius [μm] | 14 | 14.9–22.5 | 17.8 ± 2.4 |
| Inner lens radius [μm] | 15 | 7.2–11.8 | 9.5 ± 1.6 |
| Crystalline cone length [μm] | 23 | 23.1–33.4 | 28.0 ± 2.9 |
| Rhabdom [μm] | | | |
| Diameter CS 48–54 | 50 | 1.3–1.9 | 1.6 ± 0.01 |
| Diameter CS 114–120 | 10 | 0.8–0.9 | 0.9 ± 0.1 |
| Length | 8 | 54.6–73.4 | 69.6 ± 3.0 |

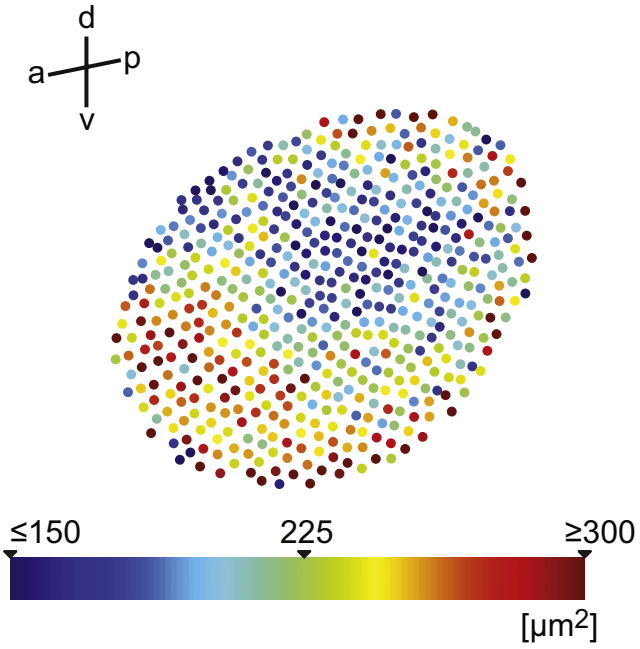


**Fig. 4.** Eye map of a left compound eye with facet areas and distribution. Facets with larger areas are located more towards the anterior frontal region of the eye. Eye orientation is defined by the insert on the top left with a: anterior, p: posterior, v: ventral and d: dorsal. Facet area was determined for the complete hexagonal shape of lenses.

the midline, mean facet diameters in the anterior part of the eye are 17.5μm ± 0.09, $n = 10$; in the lateral part 15.3 μm ± 0.14, $n = 10$ and in the posterior part 12. 8 μm ± 0.20, $n = 10$ (as measured from the eye map in Fig. 4). Using these values together with our measurements of the local eye radius we arrive at average interommatidial angles $\Delta\phi$ of 6.4° in the front, 4.9° in the lateral part of the eye and 3.0° in the back. With 30 ommatidia along the eye equator this would give each eye a horizontal visual field of approximately 150°, although the visual field will differ in workers of different body sizes, as the number of ommatidia vary with head size (Fig. 3D).

To determine the acceptance angle of the rhabdom $\Delta\rho_{rh}$, we measured the radius of the lens surface $r_1 = 17.8$ μm (SD 2.4 μm, $n = 14$), the radius of the back surface of the lens $r_2 = 9.5$ μm (SD 1.6 μm, $n = 15$) and the thickness of the lens $t = 18.7$ μm (SD 1.1 μm, $n = 25$). The focal length of the facet lens as determined by the thick lens equation (see Methods and Fig. 5) lies between 30.3 μm and 32.7 μm, depending on the refractive index of the lens of $n_1 = 1.45$ or 1.43, respectively.[1] Given the average length of the crystalline cone of 28.0 μm (SD 2.9 μm, $n = 23$), this places the image plane (marked by crosses in Fig. 5) very close to the distal tip of the rhabdom. With the average rhabdom diameter of 1.6 μm (Table 1), we find $\Delta\rho_{rh} = 2.8°–3.0°$. The average diameter of the lens blur circle at half-width is $\Delta\rho_l = 2.3°$, varying from 1.6° to 2.6° from front to back at the eye equator.

### 3.4. Histology of the compound eye

*M. bagoti* ommatidia are of the typical apposition compound eye type with a biconvex corneal lens, a crystalline cone that connects directly to the fused rhabdom. Crystalline cones and the distal tips of the rhabdoms are surrounded by dense screening pigment residing in primary and secondary pigment cells (Fig. 7) and at least in their distal part, retinula cells are densely packed with screening pigment that hugs the clear vacuole palisade around the rhabdom (Fig. 6). The rhabdom is formed by retinula cells arranged radially around the rhabdom axis (Fig. 6). The mean thickness of the corneal lenses is 18.7 μm (SD: 1.1, $N = 25$, range: 15.7–21.1 μm), the mean length of the crystalline cones is 28.0 μm (SD: 2.9, $N = 23$, range: 23.1–33.4 μm) (Table 1) and the diameter of the distal rhabdoms range from 1.3 to 1.9 μm with an average of 1.6 μm (SD: 0.01, $N = 50$, depth of section from the cornea surface: 48–54 μm). However, the rhabdoms appear to taper proximally, with an average diameter of 0.85 μm in a deeper section (114–120 μm) which is significantly different from more distal sections ($t$ test, $p < 0.001$). Rhabdoms are on average 69.6 μm long, but range from 54.6 to 73.4 μm (Table 1), with the frontal rhabdoms being the longest (Fig. 7).

## 4. Discussion

*M. bagoti* ants possess typical apposition compound eyes. The presence of a biconvex corneal lens, the arrangement of crystalline cones, primary and secondary pigment cells and retinula cells, which form the fused rhabdom, all resemble the basic structure of apposition compound eyes in hymenoptera (Varela and Porter, 1969; Land and Fernald, 1992; Brunnert and Wehner, 1973).

There is a distinct worker size polymorphism in *M. bagoti* and the dimensions of compound eyes as well as the median ocellus increase with head size (Fig. 3A–C) as do facet numbers (Fig. 3D). This is similar to other ants, such as leafcutter ants (*Atta* spp.) and fire ants (*Solenopsis* spp.), where the compound eye area and the number of ommatidia clearly scale with body size (Moser et al., 2004; Baker and Ma, 2006). Larger ants thus have better resolution. Whether visual field size also scales with body size remains unclear. In *Cataglyphis* ants, at least, the extent of the visual field does not vary with the ants' body size (Zollikofer et al., 1995) and consequently in smaller ants, resolution is reduced because less

[1] Note that we assume both the lens and the crystalline cone to have a homogeneous refractive index, although we do not know whether this is true or not. Modelling the effects of a refractive index gradient by increasing the refractive index of the lens shifts the nodal point slightly towards the front of the lens while decreasing the focal length significantly and thus moving the focal plane away from the distal tip of the rhabdom. The fact that our modelling places the focal plane at the distal tip of the rhabdom does suggest that the assumption of homogeneous refractive index provides a good approximation to the properties of the *M. bagoti* optical train.

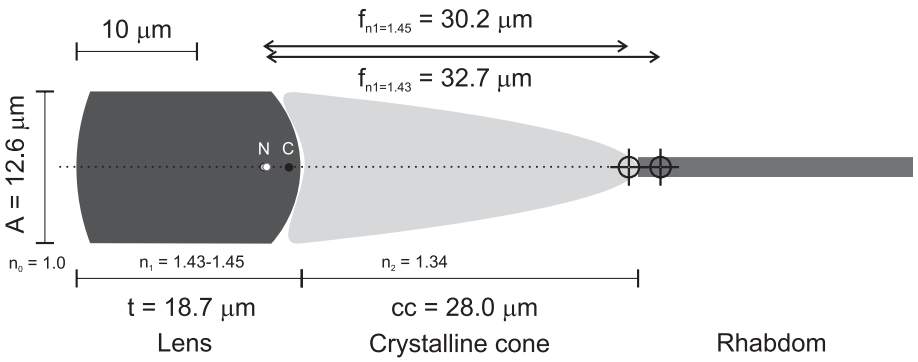


**Fig. 5.** Optical modelling of the lens-crystalline cone arrangement in the *M. bagoti* eye. See Methods for details. The focal length ($f$) was determined assuming a refractive index of the lens of both $n_1 = 1.43$ and 1.45. Crosses mark the back focal points. (N) marks the location of the secondary nodal point; (C) the location of the centre of curvature of the outer lens surface, (CC) is the crystalline cone and (A) the lens diameter. All other conventions as in Fig. 1B.

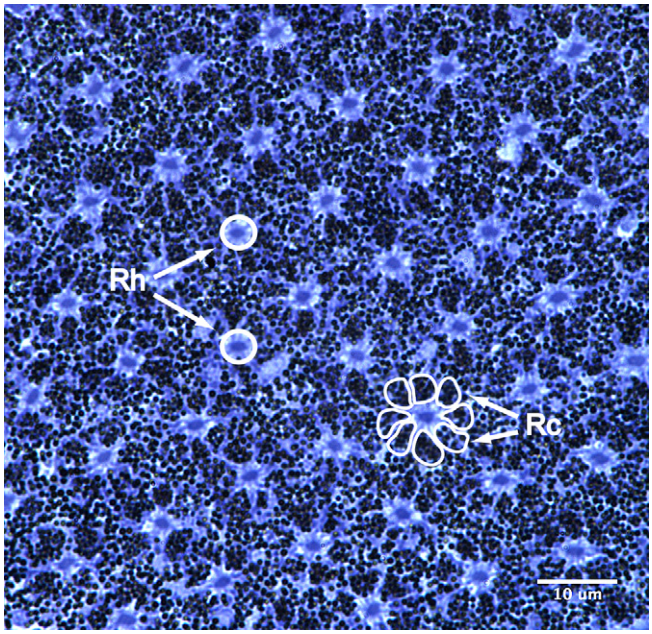


**Fig. 6.** Cross section through several ommatidia at the level of the distal rhabdom (depths of section 48–54 μm below the cornea). Rh: rhabdoms and Rc: retinula cell bodies with pigment granules.

ommatidia cover the same visual field. For *Cataglyphis* ants a large visual field appears to be more important, possibly in the context of navigation, than high resolving power (Wehner, 1983; Zollikofer et al., 1995). We estimated the horizontal extent of the visual field for each compound eye *M. bagoti* to be about 150°, but this will depend on size. It is not clear how the visual field size may affect the navigational use of the landmark panorama in different sized ants (Narendra, 2007b; Graham and Cheng, 2009a)

The sampling resolution of *M. bagoti* ($\Delta\phi = 3.7°$) is comparable to the North African desert ant, *Cataglyphis bicolor*, with average interommatidial angles ($\Delta\phi$) measuring between 3.0 and 5.0° (Zollikofer et al., 1995). This resolution is sufficient to resolve important features of the landmark panorama, as the image of a typical habitat of *M. bagoti* in Fig. 8B shows which we low-pass filtered with a Gaussian of half-width of 4° that roughly approximates the ants sampling array ($\Delta\phi$), but ignores the effects of the much smaller acceptance functions of rhabdoms. The ants' view looks blurred to the human eye but the position and shape of individual landmarks are clearly resolvable and can be used for orientation and navigation.

The ratio of the acceptance angle $\Delta\rho_{rh}$ to the interommatidial angle $\Delta\phi$ is 0.8° in *M. bagoti*, much less than the optimal 2, which implies severe under-sampling of the image while providing high contrast (Land, 1997; Smolka and Hemmi, 2009). Facet diameters are slightly larger in the anterior frontal region of the compound eye (up to 19 μm in large ants and 13 μm in small ones), compared to the smallest diameters (13 μm in large and 8 μm in small ants) we measured in the rest of the eye, which may improve, all other aspects being equal, light sensitivity and potentially also resolution

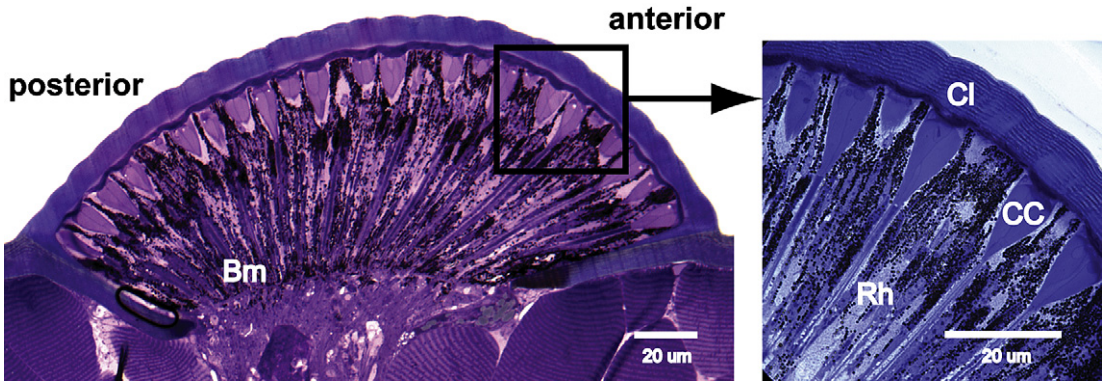


**Fig. 7.** Horizontal section through the left eye showing longitudinal organization of ommatidia. Cl: Corneal lens, CC: crystalline cone, Rh: rhabdom and Bm: basal membrane. Close-up cut-out shows the multilayered and biconvex lens.

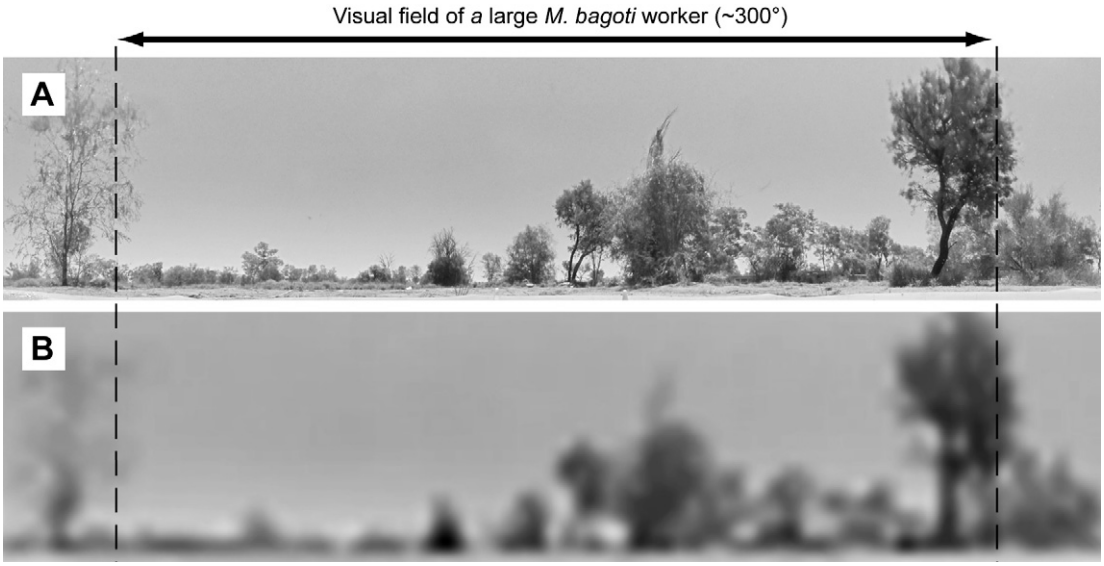


**Fig. 8.** Panoramic photograph (360°) of a typical habitat of *M. bagoti* (Alice Springs, NT) with an unmodified view of the panorama, skyline and proximate and distal landmarks (A). (B) Low-pass filtered image with an indicated horizontal field of view of 300° and a sampling resolution of 4° of a large worker.

by 50%, compared to the rest of the eye. In the North African desert ant *C. bicolor* an area of increased spatial resolution lies along the eye equator and has been called the foveal belt (Zollikofer et al., 1995). Such equatorial acute zones or visual streaks are typical for animals that inhabit flat, featureless environments (Hughes, 1977; Zeil et al., 1989; Smolka and Hemmi, 2009) while the compound eye organization of *M. bagoti*, in contrast, appears to have been shaped by a need for improved contrast sensitivity in the direction of heading.

In addition to the compound eyes, workers of *M. bagoti* possess three ocelli. In ants, ocelli are rarely present in the pedestrian workers, but are regularly found in flying alates (Hölldobler and Wilson, 1990). The small size of the ocelli in *M. bagoti* is typical for insects with diurnal lifestyle (Warrant et al., 2006; Narendra et al., 2010), where they are thought to play an important role in the control of roll and pitch movements of the head (Krapp, 2009). In *Cataglyphis* ants, ocelli provide (in addition to the specialised dorsal rim area) celestial compass information (Fent and Wehner, 1985) and it will be interesting to explore whether this is also the case in *M. bagoti*.

## Acknowledgements

We are grateful for facilities provided by the Centre for Advanced Microscopy at The Australian National University, Canberra and the ARC Centre of Excellence in Vision Science. SS was supported by a Macquarie University graduate scholarship, Sydney. AN was supported by a postdoctoral fellowship from The Australian Research Council (DP0986606). AN and JZ acknowledge additional support from the ARC Centre of Excellence in Vision Science. We thank Antoine Wystrach for providing us with the photographs shown in Fig. 8 and Doekele Stavenga for advice on optical modelling.

## References

Baker, G.T., Ma, P.W.K., 2006. Morphology and number of ommatidia in the compound eyes of *Solenopsis invicta, Solenopsis richteri*, and their hybrid (Hymenoptera: Formicidae). Zoologischer Anzeiger 245, 121–125.

Beugnon, G., Chagné, P., Dejean, A., 2001. Colony structure and foraging behavior in the tropical formicinae ant, *Gigantiops destructor*. Insectes Sociaux 48, 347–351.

Bregy, P., Sommer, S., Wehner, R., 2008. Nest-mark orientation versus vector navigation in desert ants. The Journal of Experimental Biology 211, 1868–1873.

Brunnert, A., Wehner, R., 1973. Fine structure of light- and dark-adapted eyes of desert ants, *Cataglyphis bicolor* (Formicidae, Hymenoptera). Journal of Morphology 140, 15–19.

Çamlitepe, Y., Stradling, D.J., 1995. Wood ants orient to magnetic fields. Proceedings of the Royal Society of London B 261, 37–41.

Christian, K.A., Morton, S.R., 1992. Extreme thermophilia in a central Australian desert ant, *Melophorus bagoti*. Physiological Zoology 65, 885–905.

Collett, T.S., 1992. Landmark learning and guidance. Philosophical Transactions of the Royal Society B: Biological Science 337, 295–303.

Collett, M., Collett, T.S., 2000. How do insects use path integration for their navigation? Biological Cybernetics 83, 245–259.

Collett, T.S., Dillmann, E., Giger, A., Wehner, R., 1992. Visual landmarks and route following in desert ants. Journal of Comparative Physiology A 170, 435–442.

Duelli, P., Wehner, R., 1973. The spectral sensitivity of polarized light orientation in *Cataglyphis bicolor* (Formicidae, Hymenoptera). Journal of Comparative Physiology A 86, 37–53.

Fent, K., Wehner, R., 1985. Ocelli: a celestial compass in the desert ant *Cataglyphis*. Science 228, 192–194.

Fukushi, T., 2001. Homing in wood ants, *Formica japonica*: use of the skyline panorama. The Journal of Experimental Biology 204, 2063–2072.

Graham, P., Cheng, K., 2009a. Ants use the panoramic skyline as a visual cue during navigation. Current Biology 19, 935–937.

Graham, P., Cheng, K., 2009b. Which portion of the natural panorama is used for view-based navigation in the Australian desert ant? Journal of Comparative Physiology A 195, 681–689.

Graham, P., Fauria, K., Collett, T.S., 2003. The influence of beacon-aiming on the routes of wood ants. The Journal of Experimental Biology 206, 535–541.

Hölldobler, B., 1980. Canopy orientation: a new kind of orientation in ants. Science 210, 86–88.

Hölldobler, B., Wilson, E.O., 1990. The Ants. The Belknap Press of Harvard University Press, Cambridge, Massachusetts.

Hughes, A., 1977. The topography of vision in mammals of contrasting life style: Comparative optics and retinal organization. In: Crescitelli, F. (Ed.), Handbook of sensory physiology, vol. VII/5. Springer, Berlin Heidelberg New York, pp. 613–756.

Kohler, M., Wehner, R., 2005. Idiosyncratic route-based memories in desert ants, *Melophorus bagoti*: how do they interact with path-integration vectors? Neurobiology of Learning and Memory 83, 1–12.

Krapp, H.G., 2009. Ocelli. Current Biology 19, 435–437.

Land, M.F., 1997. Visual acuity in insects. Annual Review of Entomology 42, 147–177.

Land, M.F., Fernald, R.D., 1992. The evolution of eyes. Annual Review of Neuroscience 15, 1–29.

Land, M.F., Nilsson, D.E., 2002. Animal Eyes. Oxford University Press, Oxford.

Macquart, D., Garnier, L., Combe, M., Beugnon, G., 2006. Ant navigation *en route* to the goal: signature routes facilitate way-finding of *Gigantiops destructor*. Journal of Comparative Physiology A 192, 221–234.

Moser, J.C., Reeve, J.D., Bento, J.M.S., Lucia, T.M.C.D., Cameron, R.S., Heck, N.M., 2004. Eye size and behaviour of day- and night-flying leafcutting ant alates. Journal of the Zoological Society of London 264, 69–75.

Muser, B., Sommer, S., Wolf, H., Wehner, R., 2005. Foraging ecology of the thermophilic Australian desert ant, *Melophorus bagoti*. Australian Journal of Zoology 53, 301–311.

Narendra, A., 2007a. Homing strategies of the Australian desert ant *Melophorus bagoti* I. Proportional path-integration takes the ant half-way home. The Journal of Experimental Biology 210, 1798–1803.

Narendra, A., 2007b. Homing strategies of the Australian desert ant *Melophorus bagoti* II. Interaction of the path integrator with visual cue information. The Journal of Experimental Biology 210, 1804–1812.

Narendra, A., Si, A., Sulikowski, D., Cheng, K., 2007. Learning, retention and coding of nest-associated visual cues by the Australian desert ant, *Melophorus bagoti*. Behavioral Ecology and Sociobiology 61, 1543–1553.

Narendra, A., Reid, S.F., Greiner, B., Peters, R.A., Hemmi, J.M., Ribi, W.A., Zeil. J. 2010. Caste-specific visual adaptations to distinct daily activity schedules in Australian Myrmecia ants. Proceedings of the Royal Society of London B (doi:10.1098/rspb.2010.1378).

Ribi, W., Engels, E., Engels, W., 1989. Sex and caste specific eye structure in stingless bees and honeybees (Hymenoptera: Trigonidae, Apidae). Entomologia Generalis 14, 233–242.

Riveros, A.J., Srygley, R.B., 2008. Do leafcutter ants, *Atta colombica*, orient their path integrated home vector with a magnetic compass? Animal Behaviour 75, 1273–1281.

Sabatini, D.D., Bensch, K., Barrnett, R.J., 1963. Cytochemistry and electron microscopy. The Journal of Cell Biology 17, 19–58.

Schultheiss, P., Schwarz, S., Wystrach, A., 2010. Nest relocation and colony founding in the Australian desert ant *Melophorus bagoti* Lubbock (Hymenoptera: Formicidae). Psyche (Article ID: 435838).

Smolka, J., Hemmi, J.M., 2009. Topography of vision and behaviour. The Journal of Experimental Biology 212, 3522–3532.

Stavenga, D.G., 2003a. Angular and spectral sensitivity of fly photoreceptors. I. Integrated facet lens and rhabdomere optics. Journal of Comparative Physiology A 189, 1–17.

Stavenga, D.G., 2003b. Angular and spectral sensitivity of fly photoreceptors. II. Dependence on facet lens F-number and rhabdomere type in *Drosophila*. Journal of Comparative Physiology A 189, 189–202.

Varela, F.G., Porter, K.R., 1969. Fine structure of the visual systems of the honeybee (*Apis mellifera*). Journal of Ultrastructure Research 29, 236–259.

Warrant, E.J., Kelber, A., Wallén, R., Wcislo, W.T., 2006. Ocellar optics in nocturnal and diurnal bees and wasps. Arthropod Structure & Development 35, 293–305.

Wehner, R., 1983. Taxonomie, Funktionsmorphologie und Zoogeographie der saharischen Wüstenameise *Cataglyphis fortis* (Forel 1902) stat. nov. (Insecta: Hymenoptera: Formicidae). Senckenbergiana Biologica 64, 89–132.

Wehner, R., 2003. Desert ant navigation: how miniature brains solve complex tasks. Journal of Comparative Physiology A 189, 579–588.

Wehner, R., Müller, M., 2006. The significance of direct sunlight and polarized skylight in the ant's celestial system of navigation. Proceedings of the National Academy of Science of the USA 103, 1275–1279.

Wehner, R., Räber, F., 1979. Visual spatial memory in desert ants, *Cataglyphis bicolor* (Hymenoptera: Formicidae). Experientia 35, 579–588.

Wystrach, A., Schwarz, S., Schultheiss, P., Beugnon, G., Cheng, K., 2010. Views, landmarks, and routes: how do desert ants negotiate an obstacle course? Journal of Comparative Physiology A (doi: 10.1007/s00359-010-0597-2).

Zeil, J., Nalbach, G., Nalbach, H.-O., 1989. Spatial vision in a flat world: Opti cal and neural adaptations in arthropods. In: Singh, R.N., Strausfeld, N.J. (Eds.), Neurobiology of sensory systems. Plenum Press, New York, pp. 123–137.

Zollikofer, C.P.E., Wehner, R., Fukushi, T., 1995. Optical scaling in conspecific *Cataglyphis* ants. The Journal of Experimental Biology 198, 1637–1646.